4 DES and its modifications and enhancements

A. Garbaruk, M. Shur, M.Strelets, A. Travin (NTS)

Abstract

The present chapter briefly summarises a progress in DES modelling reached in the course of DESider. Introduction outlines a motivation for development of the hybrid RANS-LES methods, in general, and a place of DES and DES-like models within this rather wide group of turbulence resolving approaches, particularly. Then, in Section 4.2, the original DES formulation is presented together with a general approach to building DES versions based on different background RANS models and a list of such versions used or developed in DESider. Finally, Sections 4.3, 4.4 describe two more general modifications not related to any specific background model and touching upon the basics of DES. They are Delayed DES (DDES) and Improved DDES (IDDES), which permit to eliminate major flaws of the "standard" DES found in the course of its intensive use both within and outside DESider and, also, to widen an area of DES and DES-like models applicability.

4.1 Introduction

It is currently commonly accepted that a wide range of wall-bounded flows with massive separation being of primary importance for aeronautic industry cannot be quantitatively predicted in a reliable way by classical RANS models of *any level of complexity*, including non-linear eddy viscosity models and DRSM. On the other hand, approaches based on "first principles", i.e., DNS and LES, which are now considered as quite capable of facing this challenge, are still computationally non-affordable at practical Reynolds numbers and will probably remain such during a major part of this century, even based on a very optimistic prognosis regarding computer power increase. This situation stimulated intensive work on development of hybrid, RANS-LES, approaches whose appearance at the end of the 20th century can be considered to a certain extent as a "turning-point" in a view on turbulence modelling and simulation strategies. These approaches plausibly combine the advantages of RANS and LES and can therefore serve as a valuable addition to pure RANS in the arsenal of industrial computational tools until LES and DNS become manageable.

DES proposed in Spalart et al., 1997 is historically the first approach of such a type. Its general idea is to combine the fine-tuned RANS technology in the attached boundary layers with the "raw power" of LES in the separated flow regions populated with relatively large and more geometry-specific "detached" eddies whose representation is beyond the capabilities of the traditional RANS models. Implementation of this idea is gratifyingly simple. It is based on using the same background RANS model with different length scales (RANS and sub-grid ones respectively) depending on the local grid-resolution. Exactly this simplicity and also impressive results obtained in the first uses of DES for the complex aerodynamic applications by its authors (see, for example, Shur et al., 1999,

Travin et al., 2000, Strelets, 2001) and positive experience accumulated in the course of FLOMANIA project (Haase et al., 2006) have motivated further development and assessment of this approach in DESider.

In Sections 4.3 and 4.4 below we present a major outcome of this effort, namely, newly proposed modifications of DES (Delayed DES or DDES and Improved DDES or IDDES). The first one eliminates the odd reaction of the original DES (hereafter DES97) to a grid-refinement beyond some limit ("Model-Stresses Depletion" (MSD) or "Grid-Induced Separation" (GIS)), whereas the second extends the DES-like formalism to Wall Modelling LES (WMLES) and, therefore, significantly broadens DES ranges of applicability. However before this, in Section 4.2, we concisely outline the DES97 formulation and a general methodology used for building its versions based on other than Spalart-Allmaras background turbulence models.

4.2   DES97 formulation and general principles of building DES models based on different RANS models

DES97 combines the S-A RANS model with its Sub-Grid Scale (SGS) "counterpart" by means of the "DES limiter" defined by

$$l_{DES} = \min\{d_w, C_{DES}\Delta\}, \tag{4.1}$$

where l_{DES} is the model length scale, d_w is the distance to the wall involved in the destructive term of the S-A model, C_{DES} is the only additional empirical model constant, and Δ is defined as the largest local grid-spacing:

$$\Delta = \max\{\Delta_x, \Delta_y, \Delta_z\}. \tag{4.2}$$

Substituting of the length scale (4.1) in place of the distance to the wall in the eddy-viscosity transport equation of the S-A RANS model directly results in the DES97 model, which performs as the background RANS model in the attached boundary layer (at $d_w < C_{DES}\Delta$) and as an SGS model with "implicit filter" $C_{DES}\Delta$ in the separation flow region away from the walls ($d_w > C_{DES}\Delta$).

A more general definition of the DES limiter (4.1) compatible with any RANS model given by Travin et al., 2002 reads as

$$l_{DES} = \min\{l_{RANS}, l_{LES}\}, \tag{4.3}$$

where l_{RANS} is the RANS length scale explicitly or implicitly involved in any RANS model (e.g., for the k-ω model this length scale is defined as $l_{RANS} = k^{1/2}/(C_\mu\omega)$, and for the k-ε model $l_{RANS} = k^{3/2}/\varepsilon$) and $l_{LES} = C_{DES}\Delta$ is the LES length scale.

Note that in accordance with the definition (4.1), location of the RANS-LES interface depends only upon the grid used in the simulation, whereas with the definition (4.3) it may become also solution-dependent. Other than that, the latter definition provides some "freedom of choice" regarding specific terms of RANS

model equations in which the RANS length scale should be replaced by the DES one. The only "guideline" for this suggested in Travin et al., 2002 is that at the equilibrium ("generation is equal to dissipation"), resulting SGS model should reduce to the Smagorinsky model. This question was thoroughly studied by TUB in the course of DESider and is discussed in detail in Yan et al., 2005. Leaving aside these "subtleties", (4.3) suggests a straightforward procedure for building a DES model based on arbitrary RANS model. This resulted in a wide set of DES versions based on RANS models ranging from one- and two-equations linear eddy viscosity models (e.g., S-A and Menter SST k-ω models) to algebraic Reynolds stress models (e.g., CEASM of Lübcke et al., 2002). A list of such models used/developed in DESider is presented in Table 1. Their formulations can be found in the FLOMANIA final report (Haase et al., 2006) and / or in the original publications.

The DES models with the low Reynolds number correction appeared in the Table include a modified expression for the LES length scale needed to compensate activation of the low-Reynolds number terms of a background RANS models in the LES mode. It reads as:

$$l_{LES} = \Psi C_{DES} \Delta , \qquad (4.4)$$

where the function Ψ depends on the ratio of the eddy and molecular viscosities and deviates from the value of 1.0 only at low sub-grid viscosities (see Shur et al., 2003, Spalart et al., 2006, Mockett et al., 2007). For RANS models not containing any low-Reynolds number terms (e.g., the Menter SST model), Ψ is equal to 1.

As of today, no strong evidences of noticeable DES model-sensitivity for the wall-bounded flows are known (this is supported also by new results presented in Chapter IV of this book). This is naturally considered as an essential advantage of DES. Nonetheless, its versions based on different RANS models, including RSM ones, are still of interest, at least for two reasons. The first one is that some of these versions may surpass the S-A or even M-SST-based DES in the flows with non-fixed turbulent separation which prediction is a responsibility of the RANS-branch of DES. The second not less important motivation for development of such DES-versions is caused by "personal affections" of different research groups and aeronautical industries to this or that RANS turbulence model. Whether objective or not, this makes it logical to have a DES version based exactly on those models which are used in the RANS context. A straight example of this practice is the DES-version developed in the course of DESider by Dassault Aviation and based on two-layer SST k-ε RANS model: this model is routinely used by the company as a reference RANS model providing for a fairly good accuracy in most of typical applications it deals with.

Table 1 DES versions based on different RANS models used/developed in DESider

Acronym	Background RANS model	References
S-A DES (DES97)	S-A model, Spalart and Allmaras, 1994	Spalart et al., 1997
SAE-DES	S-A model with Edwards and Chandra, 1996, modification	-
SALSA DES	Strain-Adaptive Linear S-A model, Rung et al., 2003	Bunge et al., 2007
S-A DES with low-Re correction	S-A model	Shur et al., 2003, Spalart et al.. 2006
SAE and SALSA DES with low-Re correction	SAE and SALSA models	Mockett et al., 2007
M-SST DES	k-ω Shear Stress Transport model, Menter (1993)	Travin et al., 2002
WCX k-ω DES	k-ω model, Wilcox, 1988	Yan et al., 2005
LLR k–ω DES	Linear Local Realisable k–ω model, Rung and Thiele, 1996	Bunge et al., 2007
X-LES	TNT k-ω model, Kok, 2000	Kok et al., 2004
k-DES	Modified Chen-Patel k-equation model, Chen and Patel, 1988	Peng, 2006
k-ε DES	Two-Layer SST k-ε Chalot et al., 1994	-
CEASM DES	Compact Explicit Algebraic Stress model, Lübcke et al., 2002	Bunge et al., 2007
OES DES	k-ω model, Wilcox, 1988	Braza et al., 2006 Elakoury et al., 2007
Zonal S-A DES	S-A model	Deck, 2005
DDES	Any background model	Spalart et al., 2006
S-A and M-SST IDDES	S-A and Menter SST models	Travin et al., 2006
SAE and CEASM IDDES	SAE and CEASM models	Mockett et al., 2007

4.3   DDES

4.3.1 *Motivation and objective*

DES97 is well understood in thin boundary layers with flattened grid cells, where it functions in the RANS mode, and in regions of massive separation with grid cells close to isotropic, where it performs in LES mode. However DES can exhibit an incorrect behaviour in thick boundary layers and shallow separation regions. This behaviour begins when the grid spacing parallel to the wall, $\Delta_\parallel$, becomes less than the boundary-layer thickness. The grid spacing is then fine enough for the DES length-scale to follow the LES branch in accordance with (4.1) and, therefore, lower the eddy viscosity below the RANS level. However resolved

Reynolds stresses deriving from velocity fluctuations ("LES content") have not yet replaced the modelled Reynolds stresses with this grid. The depleted stresses reduce the skin friction, which can even lead to premature or Grid Induced Separation (GIS).

To elucidate this issue, Fig. 1 displays three types of grid in a boundary layer. Recall that DES97 is designed to treat the *entire* boundary layer using a RANS model and to apply LES *only* to separated regions.

In the Type I grid, typical of RANS and of DES with a thin boundary layer, the wall-parallel spacings, $\Delta_\parallel$, set Δ via (4.2) and exceed δ, so that the DES length-scale is on the "RANS branch" ($l_{DES} = d_w$) throughout the boundary layer. The model functions as intended, since DES was created precisely to by-pass LES in large areas of thin boundary layer.

The other extreme is the Type III, LES grid, with all spacings much smaller than δ. The model functions as an SGS model (i.e., $l_{DES} = C_{DES}\Delta$) over the bulk of the boundary layer, and as a RANS-like model $l_{DES} = d_w$ very near the wall, with a "grey" layer in-between. This regime presents using the DES formalism for WMLES and is considered in Section 4.4 below.
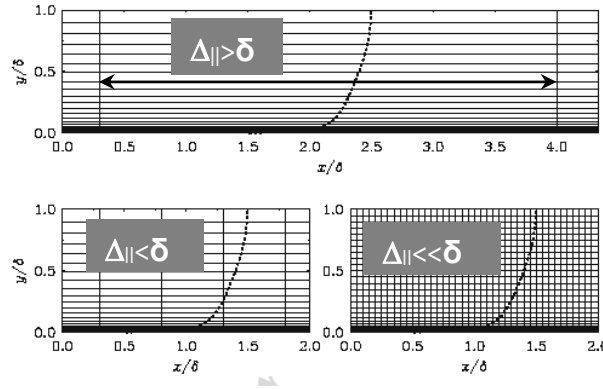

Figure 1 Grids in a boundary layer. Top – Type 1, natural DES; left - Type II, ambiguous spacing; right - Type III, LES grid. Dashed lines – mean velocity profile. δ is the boundary layer thickness. Assume $h_z \sim h_x$

The "ambiguous" grid of the Type II unfortunately activates the LES mode of DES ($l_{DES} = C_{DES}\Delta$) deep inside the boundary layer, but is patently not fine enough to support resolved velocity fluctuations, i.e., LES content. This results in a reduction of the eddy viscosity, and therefore the modelled Reynolds stresses, without any sizeable resolved stresses to restore the balance. The effect is referred to as Modelled Stress Depletion (MSD). It may occur either when the grid is gradually refined starting from the Type I, typically when a user is justifiably seeking grid convergence, or when geometry features demand a fine wall-parallel

grid, or when a boundary layer thickens and nears separation. For instance, over an airfoil, the same grid may be of the Type I near its leading edge and of the Type II close to the trailing edge.

The MSD was predicted by Spalart et al., 1997 from the origin of DES97, though anticipated only with "excessive" grid refinement and therefore not perceived as a major issue. However, later on it was encountered in studies of Caruelle, 2000 and Deck, 2002, and strongly emphasized by Menter and Kuntz, 2004 who showed how severe cases of MSD lead to GIS, although with 2D examples which were somewhat artificial. Further studies have shown that 3D grids quite affordable today can lower $\Delta_\parallel$ sufficiently to result in MSD, which motivated a search of the ways to eliminate it.

4.3.2 DDES formulation

The first proposal on eliminating MSD was that of Menter and Kuntz, 2004, who suggested using the F_1 or F_2 functions of the SST k-ω model of Menter, 1993 to identify the boundary layer and prevent a premature switch of DES to LES mode within it. Then a more general approach, Delayed DES or DDES, was developed (Spalart et al., 2006), which is a derivative of the Menter and Kuntz proposal applicable to any RANS model. Its formulation is presented below.

The argument of the blending functions F_1 and F_2 of the SST k-ω model, $\sqrt{k}/(\omega d_w)$, is the ratio between the internal length scale $\sqrt{k}/\omega$ of the k-ω turbulence model and the distance to the wall. Both functions equal 1 in the boundary layer, and fall to zero rapidly at its edge. One-equation models, such as the S-A one, do not have an internal length-scale, but involve the parameter r, which is also the ratio (squared) of a model length-scale to the wall distance. Exactly this, slightly modified, parameter is used for building DDES approach:

$$r_d \equiv \frac{\nu + \nu_t}{\sqrt{U_{i,j} U_{i,j}}\, \kappa^2 d_w^2} \, , \tag{4.5}$$

where ν is the molecular kinematic viscosity, ν_t is the eddy viscosity, $U_{i,j}$ are the velocity gradients, and κ is the von Kármán constant. Similar to r in the S-A model, this parameter equals 1 in a logarithmic layer, and falls to 0 gradually towards the edge of the boundary layer. The addition of ν in the numerator of (4.5) corrects the very near-wall behavior by ensuring that r_d remains away from 0. The subscript "d" represents "delayed."

The quantity r_d is used in the function:

$$f_d = 1 - \tanh[(8 r_d)^3] \, , \tag{4.6}$$

which is designed to be 1 in the LES region, where $r_d \ll 1$, and 0 elsewhere (and to be insensitive to r_d exceeding 1 very near the wall). It is similar to F_2, and rather steep near $r_d = 0.1$. The values 8 and 3 for the constants in (4.6) are based

on intuitive shape requirements for f_d, and on tests of DDES in the flat-plate boundary layer (see Spalart et al., 2006). These values ensure that the solution is essentially identical to the RANS solution, even if Δ is much less than δ (it is conceivable that models very different from S-A would make r_d approach 0 at $d_w=\delta$ differently enough to require a modest adjustment of f_d). The application of the above procedures to S-A DES proceeds by re-defining the DES length scale l_{DES} (4.1):

$$l_{DES} = d_w - f_d \max(0, d_w - C_{DES}\Delta). \qquad (4.7)$$

Although very simple in terms of coding, this new definition does not represent a minor adjustment within DES97 in terms of physics. Indeed, without it, l_{DES} (4.3) depends only on the grid, whereas the modified length-scale also depends on the eddy-viscosity field, which is time-dependent. The crucial effect is that RANS function is self-perpetuating, i.e., the model using (4.7) for l_{DES} can "refuse" LES mode if the function f_d indicates that the point is well inside a boundary layer, as judged from the value of r_d. However, if massive separation occurs, f_d does rise from 0, and LES mode takes over. In fact, the switch from RANS to LES takes place more abruptly following separation than in the DES97, which is desirable, since the grey area between RANS and LES becomes narrower. Although this does not in itself create LES content, it accelerates its growth following natural instabilities, closer to the region where modelled Reynolds stresses are still at full strength.

This behaviour is confirmed by the numerical examples presented in Chapter IV (for more recent examples, see, e.g. Trapier et al., 2008).

4.4   IDDES

4.4.1 Motivation and objective

As already mentioned, both the DES97 and DDES approaches are aimed at computing of massively separated turbulent flows. However, an attempt to apply DES formalism for WMLES in the developed channel flow undertaken by Nikitin et al., 2000 turned out generally successful in the sense that the approach enabled LES predictions at unlimited values of grid-spacing parallel to the wall (in wall units) with no impractical, "channel-friendly", steps. On the other hand, the simulations produced two logarithmic layers: the "inner" log-layer, which arises because the RANS model is constructed to provide it and the "outer" log-layer, which arises since LES is functioning well once all local grid-sizes are much smaller than the distance to the wall. Unfortunately, these two log-layers turn out to be mismatched (have different intercept) resulting in lowering the skin-friction by up to 15%-20%, missing up-to-date demands for simple flows. Considering the crucial importance of WMLES which provides huge savings of computer resources compared to the full LES of the wall bounded flows and, thus, paves the

way to its industrial applications, creating a model which would plausibly combine DDES capabilities for natural DES uses with WMLES ones is very tempting and gives a strong motivation for development of a model which would not only provide a remedy of the LLM but present a single set of formulas for both natural DES applications and their WMLES uses, so that different flows or different regions inside a single simulation over a complex geometry could be automatically treated by an optimal model. An approach, which matches these objectives developed in the course of DESider was called Improved DDES or IDDES (Travin et al., 2006). IDDES includes two branches, DDES and WMLES, and a set of empirical functions designed to obtain both correct performance from these branches themselves and their coupling providing a favourable response of the combined model as DDES or WMLES depending on the inflow (or initial) conditions used in the simulation. A separate and essential element of the proposed model is a new definition of the subgrid length-scale that includes explicit wall-distance dependence, unlike the usual LES and DES practice, which involves only the grid-spacings. Below we outline all the elements of IDDES starting from this new subgrid length-scale, which enters both of its branches.

4.4.2   IDDES formulation

Sub-grid length-scale
The issue of the optimal relation between the subgrid length-scale and grid-spacings is a general issue of any LES approach not involving an explicit filtering. It is far from trivial, especially when the computational grid is significantly anisotropic, which is typical of the wall-bounded flows. Historically, the most widely employed definition has been the cube root of the cell volume. While this is a plausibly balanced quantity, it was challenged in DES97, where the maximum of the three cell dimensions was advocated instead (see (4.2)). However neither definition is successful, if judged by a straightforward application to well-resolved LES of wall-bounded flows: the values of the SGS constants, which work well in free turbulent flows with cubic cells, are then too large. For instance, the optimal value of the Smagorinsky constant for LES of channel flow is about 0.1 if the cube root is used, or roughly half its optimal value of 0.2 for Decaying Isotropic Homogeneous Turbulence (DIHT). Using the maximum grid spacing, as in (D)DES, the difference between the optimal model constants for channel flow and DIHT is even larger. This situation cannot be considered as a satisfactory one, not only because the two types of flows demand different constants but, more importantly, because any "wall-bounded" flow becomes a "free" one away from the walls, which means that the use of any single value of the constant calibrated on this or that type of flow cannot be correct in a whole flow. This motivates a search for an alternative and more physically justified definition of the subgrid length-scale, which would not demand different SGS model constants for wall-bounded and free turbulent flows.

Since wall-proximity effects, primarily inviscid blocking, are involved, the new definition of the sub-grid length scale proposed in Travin et al., 2006 relies

not only on the cell sizes, but also explicitly includes a wall-distance dependency, i.e., has the form:

$$\Delta = f(\Delta_x, \Delta_y, \Delta_z, d_w) , \qquad (4.8)$$

where Δ is the needed sub-grid length-scale, Δ_x, Δ_y, and Δ_z are the local streamwise, wall-normal, and lateral cell sizes respectively, and d_w is the distance to the wall.

Let Δ_{free} be the infinite-d_w limit of the function $f(\Delta_x, \Delta_y, \Delta_z, d_w)$. Then, following the concept in the DES (4.2), it is set equal to the maximum local grid spacing (away from the walls, the grid for an LES should be fairly isotropic anyway, and so the impact of this specific choice is not crucial)

$$\Delta_{free} = \Delta_{max} \equiv \max\{\Delta_x, \Delta_y, \Delta_z\} . \qquad (4.9)$$

As for the behaviour of Δ in very close vicinity of the wall, it should not follow the drastic decrease of the wall-normal step typical of this region (especially at high Reynolds number) and, therefore, should depend on the wall-parallel steps only:

$$\Delta_{wall} = const(d_w) = f(\Delta_x, \Delta_z) . \qquad (4.10)$$

Assuming, finally, that between these two limiting cases Δ is a linear function of d_w and that at any distance to the wall it varies within the range $\Delta_{min} \leq \Delta \leq \Delta_{max}$, a definition of the sub-grid length-scale satisfying all the above demands is formulated as follows:

$$\Delta = \min\{\max[C_w d_w, C_w \Delta_{max}, \Delta_{wn}], \Delta_{max}\} , \qquad (4.11)$$

where Δ_{wn} is the grid step in the wall-normal direction and C_w is an empirical constant set equal to 0.15 based on a well-resolved LES of the developed channel flow (see Travin et al., 2006, Shur et al., 2008).

Figure 2 shows two possible types of variation of the sub-grid length-scale Δ defined by (4.11), normalized by the maximum grid step, across a plane channel with half-width H . The first type (solid line in Fig.2) takes place if $\Delta_{wn} \leq C_w d_w$ and, therefore, in accordance with (4.11), as long as $d_w < \Delta_{max}$, the length scale Δ remains constant equal to $C_w \Delta_{max}$. Then, once $d_w > \Delta_{max}$, it grows linearly ($\Delta = C_w d_w$) until reaching the value of Δ_{max} , and stays constant after that. The second type of Δ variation (dashed line in Fig.2) corresponds to a strong wall-normal step stretching. In this case, Δ remains constant equal to $C_w \Delta_{max}$ as long as $h_{wn} < C_w \Delta_{max}$. Then, it grows with a rate higher than C_w until reaching the value of Δ_{max} and after that, just as in the first case, remains constant. Note that this scenario is undesirable, but with any rate of wall-normal step stretching that is acceptable for an accurate LES, it still is not a disaster. For instance, for a

wall-normal step varying in accordance with a geometric series, it takes place only if the series index $k > (1 + C_w)$, i.e., if $k > 1.15$, which is very close to the maximum k values $1.2 \div 1.3$ that still provide sufficient accuracy in LES. Therefore, with any acceptable rate of growth of the wall-normal step, the difference between the two branches of (4.11) is not large.
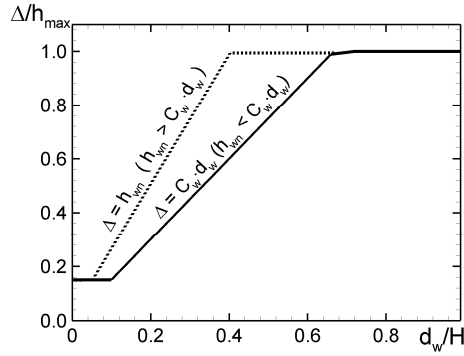

Figure 2 Two possible types of variation of the sub-grid length-scale (4.11) across the plane channel

An example demonstrating a convincing performance of the sub-grid length-scale (4.11) in the framework of pure LES is presented in Travin et al., 2006 and in Section 14 of Chapter V.

WMLES branch

This branch is intended to be active only when the inflow conditions used in the simulation are unsteady and impose some turbulent content and the grid is fine enough to resolve boundary-layer dominant eddies. It presents a new seamless hybrid RANS-LES model, which couples RANS and LES approaches via the introduction of the following blended RANS-LES length-scale:

$$l_{WMLES} = f_B(1 + f_e)l_{RANS} + (1 - f_B)l_{LES} .$$ (4.12)

In accordance with the general DES concept, in order to create a seamless hybrid model, the length-scale l_{WMLES} defined by (4.12) should be substituted into the background RANS model in place of the RANS length scale, l_{RANS}.

As far as the LES length-scale is concerned, it is defined via the sub-grid length-scale Δ (4.11) just as it is done in (D)DES (4.4).

Let us now consider two other ingredients of the length-scale (4.12), namely, the functions f_B and f_e.

The empirical blending function f_B depends upon d_w / h_{max} and is defined as

$$f_B = \min\{2\exp(-9\alpha^2), 1.0\}, \quad \alpha = 0.25 - d_w/h_{\max}. \tag{4.13}$$

It varies from 0 to 1 and provides rapid switching of the model from RANS mode (f_B=1.0) to LES mode (f_B=0) within the range of wall-distance $0.5h_{\max} < d_w < h_{\max}$ (see solid line in Fig.3).
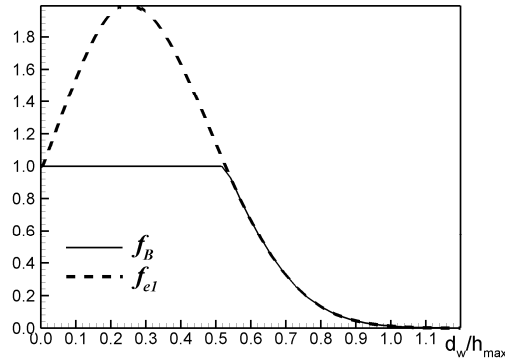

Figure 3 Profiles of the functions f_B and f_{e1} in plane channel

The second empirical function involved in (4.12), elevating function f_e, is aimed at preventing the excessive reduction of the RANS Reynolds stresses which has been observed in the interaction of the RANS and LES regions in the vicinity of their interface. It is instrumental in combating log-layer mismatch. The function f_e should be close to zero, and therefore passive, in two cases:

1. when the grid used in the simulation is sufficient for a wall-resolved LES (the RANS-LES interface is located very close to the wall, at y^+ < 15-20, so that the Reynolds stresses near the interface are negligible);

2. when the final IDDES model (see eqn. (4.22) below) effectively performs as the background RANS model (otherwise, a non-zero f_e would corrupt the correct RANS behaviour).

The function built to satisfy these demands reads

$$f_e = \max\{(f_{e1}-1),\ 0\}\Psi f_{e2}. \tag{4.14}$$

Here the functions f_{e1} is defined as

$$f_{e1}(d_w/h_{\max}) = \begin{cases} 2\exp(-11.09\alpha^2) & \textit{if} \quad \alpha \geq 0 \\ 2\exp(-9.0\alpha^2) & \textit{if} \quad \alpha < 0 \end{cases} \tag{4.15}$$

It provides a "predefined" (i.e., dependent on the grid but not on the solution) "elevating" device for the RANS component of the WMLES length-scale (4.12). As seen in Fig. 3, where f_{el} is plotted by a dashed line, it coincides with f_B when $f_B < 1$, i.e., in the transitional RANS-LES region, but then, with d_w decrease, grows up to 2.0, and then gradually falls to 1.0 on the wall.

The function f_{e2} reads:

$$f_{e2} = 1.0 - \max\{f_t, f_l\}.$$ (4.16)

It controls the intensity of "elevating" of the RANS component of the model (4.12) through the functions f_t and f_l:

$$f_t = \tanh[(c_t^2 r_{dt})^3], \quad f_l = \tanh[(c_l^2 r_{dl})^{10}],$$ (4.17)

where the quantities r_{dt} and r_{dl} are the "turbulent" and "laminar" analogues of r_d in DDES (4.5) defined by the relations

$$r_{dt} = \nu_t / \max\{[\sum_{i,j}(\partial u_i / \partial x_j)^2]^{1/2}, 10^{-10}\} \kappa^2 d_w^2,$$ (4.18a)

$$r_{dl} = \nu / \max\{[\sum_{i,j}(\partial u_i / \partial x_j)^2]^{1/2}, 10^{-10}\} \kappa^2 d_w^2,$$ (4.18b)

and c_l and c_t are additional model constants depending on the background RANS turbulence model. These constants should be adjusted so that the function f_{e2} is virtually zero when either r_{dt} or r_{dl} is close to 1.0. Similar to the parameter r_d, r_{dt} is close to 1.0 in the logarithmic part of the boundary layer, while the new parameter r_{dl}, is close to 1.0 in the laminar sublayer. So, with the properly chosen constants c_t and c_l, one of the functions, f_t or f_l is close to 1.0, and therefore the functions f_{e2} and f_e are close to zero, which ensures satisfaction of the demands 1) and 2) formulated above. Based on simulations of channel flow, the values of the constants are set to 3.55 and 1.63 for the S-A-based IDDES and 5.0 and 1.87 for the M-SST-based IDDES respectively.

Note that, in contrast to f_{el}, f_{e2} depends on the solution via the quantity $\sum_{i,j}(\partial u_i / \partial x_j)^2$ in the denominator of r_{dt} and r_{dl}. As for introducing of the function Ψ (see 4.4) into the definition of f_e (4.14), it is unrelated to the low-Re correction role this function plays in the LES mode of (D)DES, and is purely empirical. A better function to enforce the effect of f_e when the background RANS model has the low-Re terms could probably be devised. However, as shown in Section 9 of Chapter IV, even with this choice, the IDDES performance turns out quite satisfactory, so that a search for another function does not seem to be crucial.

DDES branch and its blending with the WMLES branch

This branch responsible for the DDES-like functionality of IDDES becomes active only when the inflow conditions do not have any turbulent content.

The original DDES formulation (4.7) may be presented in the following more general (applicable not only to the S-A but for any RANS background model) form:

$$l_{DDES} = l_{RANS} - f_d \max\{0, (l_{RANS} - l_{LES})\} .$$
(4.19)

Unfortunately, no way was found to blend this length-scale with that of the WMLES-branch (4.12), which would ensure an automatic choice of the WMLES or DDES mode by the final (combined) model, depending on the type of the simulation (with or without turbulent content). However this turned out to be possible with a slightly modified version of (4.19), namely,

$$\widetilde{l}_{DDES} = \widetilde{f}_d l_{RANS} + (1 - \widetilde{f}_d) l_{LES} ,$$
(4.20)

where the blending function $\widetilde{f}_d$ is defined by

$$\widetilde{f}_d = \max\{(1 - f_{dt}), f_B\} \text{ with } f_{dt} = 1 - \tanh[(8 r_{dt})^3] .$$
(4.21)

As shown in Travin et al., 2006, this definition of the length-scale is effectively equivalent to the original one in DDES (4.19).

With the use of (4.20), the required IDDES length-scale combining the WMLES and DDES scales (4.12) and (4.20) can be implemented as:

$$l_{hyb} = \widetilde{f}_d (1 + f_e) l_{RANS} + (1 - \widetilde{f}_d) l_{LES} .$$
(4.22)

Indeed, in the simulations with an inflow turbulent content, $r_{dt} \ll 1$, f_{dt} is close to 1.0, and $\widetilde{f}_d$ defined by (4.21) is equal to f_B so that (4.22) automatically reduces to (4.12). Otherwise, f_e becomes zero, and so (4.22) reduces to (4.20).

Note in conclusion that, provided that the DDES model is already available in a code, implementation of the IDDES approach, i.e., embedding the length scale (4.22) instead of DDES length-scale (4.7) is very simple. Moreover, the approach can be easily coupled with other than S-A and M-SST DES models as demonstrated by Mockett et al., 2007 who implemented SAE- and CEASM-based IDDES versions. However, in theoretical terms, the difference between DDES and IDDES is rather significant. First of all, the IDDES employs a new definition of the sub-grid length-scale that includes explicit wall-distance dependence, unlike the usual LES and (D)DES practice, which involves only the grid-spacing. Other than that, IDDES includes an additional, WMLES, branch and a set of empirical functions providing a different functionality of the combined model depending on whether a simulation does or does not have inflow turbulent content. In this sense, there is an intentional non-uniqueness of the solution within given lateral boundary conditions.

References

Braza, M., Perrin, R., Hoarau, Y. (2006). Turbulence properties in the cylinder wake at high Reynolds number. J. Fluids and Structures, Vol. 22, pp. 757–771.

Bunge, U., Mockett, C., Thiele, F. (2007): Guidelines for implementing detached-eddy simulation using different models. Aerospace Science and Technology. Vol. 11, No. 5, pp. 376-385.

Caruelle, B. (2000): Simulations d'écoulements instationnaires turbulents en aérodynamique: application à la prédiction du phénomène de tremblement. Ph.D. Thesis, INPT/CERFACS.

Chalot, F., Mallet, M., M.Ravachol, M. (1994): A comprehensive finite element Navier-Stokes solver for low-and high-speed aircraft design. AIAA Paper 94-0814.

Chen, H.C., Patel, V.C., (1988). Near-wall turbulence models for complex flows including separation. AIAA J., Vol. 26, pp.641-648.

Deck, S. (2002): Simulation numérique des charges latérales instationnaires sur des configurations de lanceur". Ph.D. Thesis, U. Orléans.

Deck, S. (2005): Numerical Simulation of Transonic Buffet over a Supercritical Airfoil. AIAA Journal. Vol. 43, pp. 1556-1566.

Edwards, J., Chandra, S. (1996): Comparison of eddy viscosity-transport turbulence models for three-dimensional, shock-separated flowfields. AIAA Journal. Vol. 34, No. 4, pp. 756–763.

Elakoury, R., Braza, M., Hoarau, Y., Vos, J., Harran, G., Sevrain, A., Unsteady flow around a NACA0021 airfoil beyond stall at 60° angle of attack. In: Procs. IUTAM Symposium on Unsteady Separated Flows and their Control, June 18-22, 2007, Corfu, Greece.

Haase, W., Aupoix, B., Bunge, U., Schwamborn, D. (editors), (2006): FLOMANIA - A European initiative on flow physics modelling. Notes on Numerical Fluid Mechanics and Multidisciplinary Design. Vol. 94, Springer-Verlag.

Kok, J.C. (2000): Resolving the dependence on freestream values for the k–ω turbulence model. AIAA Journal. Vol. 38, No. 7, pp.1292–1295.

Kok, J., Dol, H., Oskam, B., van der Ven, H. (2004): Extra-large eddy simulation of massively separated flows. AIAA paper 2004-0264.

Lübcke, H., Rung, T., Thiele, F. (2002): Prediction of the spreading mechanisms of 3D turbulent wall jets with explicit Reynolds-stress closures. In: Engineering Turbulence Modelling and Experiments 5. W. Rodi and N. Fueyo (eds), Elsevier, pp. 127–145.

Menter, F.R. (1993): Zonal two-equation k-ω turbulence models for aerodynamic flows. AIAA paper 1993-2906.

Menter, F., Kuntz, M. (2004): The Aerodynamics of Heavy Vehicles: Trucks, Buses, and Trains. Lecture Notes in Applied and Computational Mechanics, Vol. 19, chapter "Adaption of eddy-viscosity turbulence models to unsteady separated flow behind vehicles". Springer-Verlag.

Mockett, C., Greschner, B., Knacke, T., Perrion, R., Yan, J., Thiele, F. (2007): Demonstration of improved DES methods for generic and industrial applications. In: Haase, W. and Peng, S.-H. (eds.), Proceedings of Second Symposium on Hybrid RANS-LES Methods, Corfu, Greece, 17-18 June 2007.

Nikitin, N., Nicoud, F., Wasistho, B., Squires, K., Spalart, P. (2000): An approach to wall modeling in large-eddy simulations. Physics of Fluids. Vol. 12, No. 7, pp. 1629–1632.

Peng, S.-H. (2006): Towards detached eddy simulation modelling using a k-equation turbulence model. In: P. Wesseling, E. Oñate, and J. Périaux (eds), Proceedings of the

European Conference on Computational Fluid Dynamics ECCOMAS CFD 2006, Egmond aan Zee, The Netherlands.

Rung, T., Thiele, F. (1996): Computational modelling of complex boundary-layer flows. In: Proceedings of the 9th International Symposium on Transport Phenomena in Thermal-Fluid Engineering, Singapore, 1996.

Rung, U. Bunge, M. Schatz, Thiele, F. (2003): Restatement of the Spalart–Allmaras eddy-viscosity model in strain-adaptive formulation. AIAA Journal. Vol. 41, No. 7, pp. 1396–1399.

Shur, M., Spalart, P.R., Strelets, M., Travin, A. (1999): Detached-eddy simulation of an airfoil at high angle of attack. In: Rodi, W. and Laurence, D. (eds.), 4th Int. Symp. On Engineering Turbulence Modelling and Measurements, Corsica, May 24-26, 1999, pp. 669-678.

Shur, M.L., Spalart, P.R., Strelets, M., Travin, A. (2003): Modification of S-A subgrid model in DES aimed to prevent activation of the low-Re terms in LES mode. In: Proceedings of workshop on DES, St.-Petersburg, 2–3 July 2003, http://cfd.me.umist.ac.uk/flomania.

Spalart, P.R., Allmaras, S.R. (1994): A one-equation turbulence model for aerodynamic flows. La recherche aérospatiale. Vol. 1, pp. 5-21.

Spalart, P.R., Jou, W., Strelets, M., Allmaras, S. (1997): Comments on the feasibility of LES for wings, and on a hybrid RANS/LES approach. In: Advances in DNS/LES, 1st AFOSR Int. Conf. on DNS/LES, 1997.

Spalart, P.R., Deck, S., Shur, M., Squires, K., Strelets, M., Travin, A. (2006): A new version of detached-eddy simulation, resistant to ambiguous grid densities. Theoretical and Computational Fluid Dynamics. Vol. 20, pp. 181–195.

Strelets, M. (2001): Detached Eddy Simulation of massively separated flows. AIAA Paper 2001-879.

Trapier, S., Deck, S., Duveau, P. (2008): Delayed detached-eddy simulation and analysis of supersonic inlet buzz. AIAA Journal. Vol. 46, No.1

Travin, A., Shur, M., Strelets, M., Spalart, P. (2000): Detached-eddy simulations past a circular cylinder. Flow, Turbulence and Combustion. Vol. 63, pp. 293 485.

Travin, A., Shur, M., Strelets, M., Spalart, P.R. (2002): Physical and numerical upgrades in the Detached-Eddy Simulation of complex turbulent flows. In: Fluid Mechanics and its applications, Vol. 65, p. 239-254. Advances in LES of Complex Flows, R. Friedrich and W. Rodi (eds.). Proc. Of EUROMECH Colloquium 412, Kluwer Academic Publishers, Dordrecht – Boston – London.

Travin, A., Shur, M., Spalart, P.R., Strelets, M. (2006): Improvement of delayed detached-eddy simulation for LES with wall modelling. In: P. Wesseling, E. Oñate, and J. Périaux (eds), Proceedings of the European Conference on Computational Fluid Dynamics ECCOMAS CFD 2006, Egmond aan Zee, The Netherlands.

Wilcox, D. (1988): Reassessment of the scale-determining equation for advanced turbulence models. AIAA Journal. Vol. 26, pp. 1299–1310.

Yan, J., Mockett, C., Thiele, F. (2005): Investigation of alternative length scale substitutions in detached-eddy simulation. Flow, Turbulence and Combustion. Vol. 74, No. 1, pp. 85–102.